

Surface electromagnetic waves on layered systems with damping*

C. A. Ward, R. W. Alexander, and R. J. Bell

Department of Physics and Graduate Center for Materials Research, University of Missouri-Rolla, Rolla, Missouri 65401

(Received 14 July 1975)

The dispersion curves, propagation distances, and Poynting vectors of surface electromagnetic waves propagating on a system of Cu-Cu₂O-air with variable film thickness have been calculated using the full dispersion relation including damping. Double-dip structure in the propagation distance for intermediately thick overlayers, the shifting of one dip below σ_{TO} , and the presence of the other dip at σ_{LO} are explained in terms of features of the dispersion curve. The complete Poynting-vector calculations show that predictions of field bunching at σ_{LO} are probably in error.

I. INTRODUCTION

Recent theoretical studies¹ have produced a dispersion relation for surface electromagnetic waves (SEW) propagating on n -layer systems, which uses no approximations and includes damping. SEW are currently being used to study oxide overlayers, semiconductor devices, adsorbed species, adhesives, and other layered structures which require nondestructive testing techniques.²⁻⁴ The computer solutions derived from this equation are indicative of the actual experimental results to be expected in these overlayer studies.

We have investigated a system of copper⁵ overlaid with Cu₂O of varying thickness against a third layer of air (see Fig. 1) in the region of the Cu₂O transverse- and longitudinal-optical-phonon frequencies (σ_{TO} and σ_{LO}).⁶ This region was chosen because the dielectric function of the Cu₂O assumes both negative and positive values. The dispersion, $1/e$ propagation distance, and time-averaged energy flow were calculated. These three parameters will be considered separately in the following sections.

Our results show that (i) dips in the propagation distance occur at both σ_{TO} and σ_{LO} for intermediate film thicknesses; (ii) the position of the dip near σ_{TO} is a strong function of film thickness and moves significantly below σ_{TO} before returning to that frequency for an infinitely thick overlayer; (iii) approximations based on purely exponentially damped or propagating character of the wave in the direction normal to propagation in the overlayer are inaccurate if damping is included; and (iv) predicted field bunching in thin films is contrary to complete Poynting-vector calculations.

II. DISPERSION RELATION

Several solutions to the dispersion relation are to be expected for multilayer systems.^{1,4,7} For thin overlayers one solution approximates the Cu-air two-media dispersion relation, which in turn lies near the vacuum light line for infrared frequencies.⁴ This solution near the light line has

been experimentally confirmed,⁸ so this investigation will concentrate on that mode.

Figure 2 shows the dispersion relation for SEW propagating on Cu with Cu₂O overlayer thicknesses of 8000 and 10 000 Å, which are bounded on the other side by a semi-infinite air layer. The curve for a 500-Å-Cu₂O thickness lies too close to the vacuum light line to be shown in the figure. The complex dielectric functions of the Cu, Cu₂O, and air are ϵ_1 , ϵ_2 , and ϵ_3 , respectively. For convenience, the plot is divided into three frequency regions.

Region I. The condition for the existence of a surface electromagnetic wave at an interface between layers n and $n+1$ is that $\text{Re } \epsilon_n < -\text{Re } \epsilon_{n+1}$.⁹ (In the discussion immediately following, the real part of each ϵ will be assumed.) For thin films discussed above, the solution which lies near the Cu-air two-media solution will be present throughout all three regions because of the large negative dielectric function of the metal in this frequency range, and thus ϵ_1 is always less than $-\epsilon_3$ ($\epsilon_3 \approx 1$). In this region, the dielectric function of the Cu₂O, ϵ_2 , is positive, and so ϵ_1 is also less than $-\epsilon_2$. Therefore, a mode which approximates two-media dispersion exists along the Cu-Cu₂O interface. No similar mode can occur along the Cu₂O-air interface because ϵ_2 and ϵ_3 are both positive. The Cu-Cu₂O solution lies far to the right of the Cu-air solution (off scale in Fig. 2) and bends over rapidly. The result is a coupled three-media mode showing characteristics of both the Cu-air and Cu-Cu₂O modes. Therefore, three-media dispersion can be understood in terms of combinations of two-media modes between the layers.

Figure 2 also shows that as the thickness of the Cu₂O layer increases, the bending of the solution away from the vacuum light line becomes much more pronounced. This is because with the addition of Cu₂O, the Cu-Cu₂O mode associated with it becomes dominant over the Cu-air mode, and thus the coupled mode shows more strongly the bend-over characteristics.

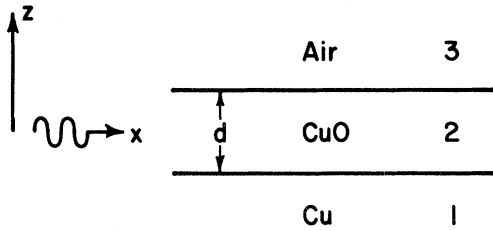


FIG. 1. Three-media system of Cu-Cu₂O-air with surface electromagnetic waves propagating in the x direction. The thickness of layer 2 is represented by d.

Region II. In this region, the dielectric function of the Cu₂O overlayer, ϵ_2 , becomes negative and less than $-\epsilon_3$. Thus, the condition for a two-media mode at the Cu₂O-air interface is met, and the departure from linearity in the dispersion relation shows coupling with this mode. Since ϵ_2 and ϵ_3 are both negative, the Cu-Cu₂O mode is not present in this region.

The amount of bending in the dispersion curve is again thickness dependent. As the Cu₂O becomes thicker, the solution loses its resemblance to the Cu-air mode and assumes the Cu₂O-air character. The effect is not as great as in region I. This

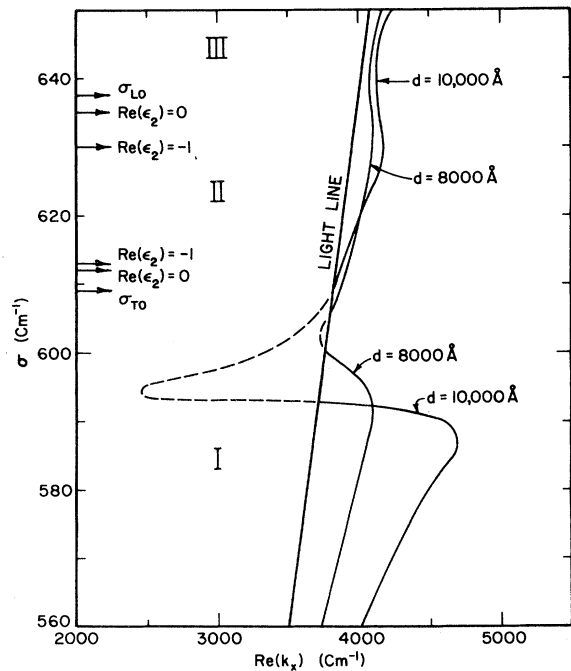


FIG. 2. Three-media dispersion curves for Cu-Cu₂O-air with Cu₂O thicknesses of 8000 and 10 000 Å compared with the vacuum light line. The Cu₂O dielectric function is positive in regions I and III and negative in region II. The values $\sigma_p = 6.5 \times 10^4 \text{ cm}^{-1}$ and $\sigma_r = 266 \text{ cm}^{-1}$ for Cu were fitted from Ref. 5. The values $\sigma_{T0} = 609 \text{ cm}^{-1}$, $\delta\epsilon = 0.63$, $\epsilon_\infty = 6.5$, and $\gamma = 18.5 \text{ cm}^{-1}$ for Cu₂O were obtained from Ref. 6.

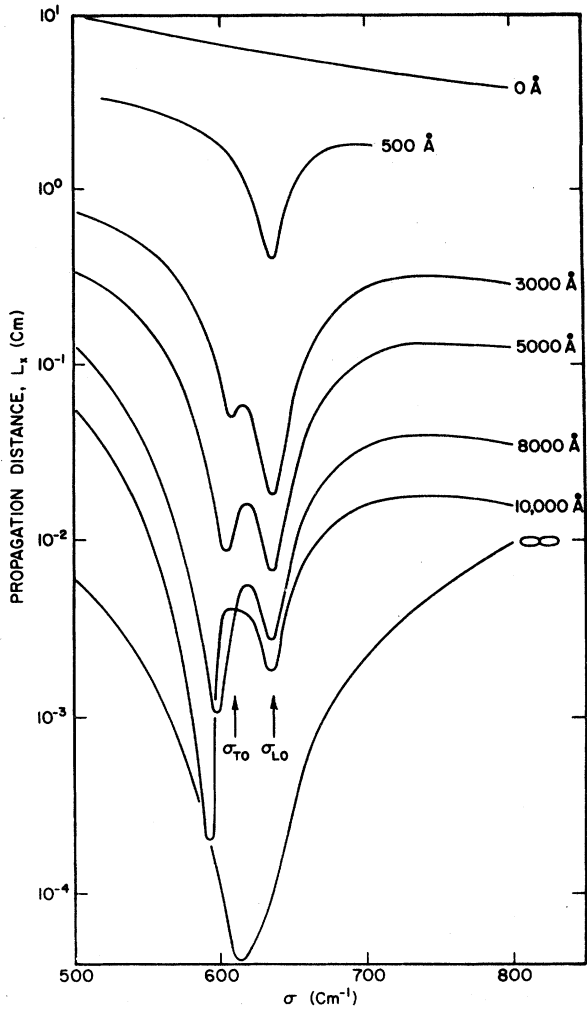


FIG. 3. Propagation distance L_x for surface electromagnetic waves as a function of frequency for various Cu₂O thicknesses for a Cu-Cu₂O-air system.

can be explained in terms of the Cu-Cu₂O and Cu₂O-air two-media modes approaching their semi-infinite limits. The extension distance of an SEW is much greater in the overlayer than in the supporting medium. In region I, the Cu₂O is the overlayer in the coupled two-media mode and an increase in thickness toward the semi-infinite limit has great effect. In region II, the Cu₂O is the supporting medium in the coupled two-media mode, and increases in thickness have small effect since the extension distance into it is comparatively small.

Region III. The dielectric function of the overlayer is again positive, and the discussion for region I is applicable.

III. PROPAGATION DISTANCE

The $1/e$ propagation distance L_x of a surface electromagnetic wave is defined as

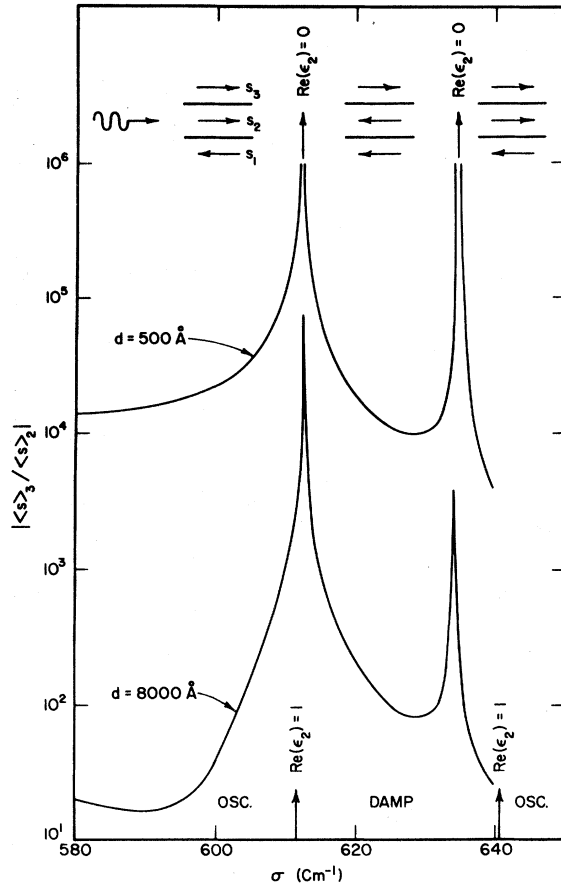


FIG. 4. Absolute value of the time-averaged energy-flow ratio of layer 3 (air) to layer 2 (Cu_2O) for Cu_2O thicknesses of 500 and 8000 Å. Also shown at the top of the figure are the directions of the SEW energy flow in the different frequency regions defined by $\text{Re}\epsilon_2 = 0$. At the bottom of the figure the primarily oscillating (osc) or exponentially damped (damp) character of k_x in layer 2 is delineated in regions bounded by $\text{Re}\epsilon_2 = 1$.

$$L_x = 1/2k_{2x} \quad (1)$$

where k_{2x} is the imaginary (damped) part of the wave vector k_x in the direction of propagation. Previous studies^{4,10} of three-layer systems have shown that for very thin overlayers a dip occurs in the propagation distance as a function of frequency near σ_{LO} of the overlayer. This is in contrast to the case of two layers, where the dip occurs at σ_{TO} .^{2,9}

Figure 3 shows the calculated propagation distance as a function of frequency using the exact equations¹ for Cu-Cu₂O-air with Cu₂O thicknesses of 0, 500, 3000, 5000, 8000, and 10000 Å and ∞. As can be seen, intermediate thicknesses produce two dips, one near σ_{TO} and the other near σ_{LO} .

The appearance of these dips can be understood through the structure of the dispersion curves discussed above. For thin layers (500 Å) the coupling of the Cu-Cu₂O and Cu-air modes in region I is negligible. However, there is some slight structure in region II, which occurs near σ_{LO} because of the sign of ϵ_2 , producing a corresponding dip in L_x . As the Cu₂O thickness is increased, structure begins to occur in region I below σ_{TO} , producing the second L_x dip.

The depth and position of each dip changes with the amount and position of bend in the dispersion curve. In region II, there is little change in the shape of the dispersion curve with thickness, hence the L_x dip changes little in position and slowly in depth. However, in region I there is a rapid change in the size and position of the dispersion-curve bendover. With increasing thickness, the bendover gets very large and shifts to lower wave number. A corresponding change occurs in the depth and position of the dip in L_x .

At an infinite overlayer thickness, a single dip in L_x appears at σ_{TO} . This is associated with the normal two-media dispersion curve for Cu-Cu₂O, which shows structure at σ_{TO} .⁹

Calculations of the dispersion curves and propagation distances for a metal-dielectric-metal system in the region of σ_{TO} and σ_{LO} for the dielectric have also been carried out. While the structure is different from that obtained in the calculations discussed above, similar interpretations can be made. Systems of four and five media are also being investigated, and the complicated structure obtained should also yield to similar analysis.

IV. POYNTING VECTOR

The equations for the time-averaged energy flow in the overlayer and in the air may be written: in the overlayer

$$\langle s \rangle_2 = -\frac{c}{8\pi} \text{Re} \int_0^d E_{2z} H_{2y}^* dz, \quad (2)$$

with

$$\int_0^d E_{2z} H_{2y}^* dz = \left[\frac{-2\pi\sigma k_x \epsilon_2^*}{|k_{2z}|^2} \right] \left\{ \frac{1}{4} \left(\frac{1}{\text{Re}k_{2z}} \sinh 2a - \frac{1}{\text{Im}k_{2z}} \sin 2b \right) + \frac{1}{4} \frac{|\epsilon_1|^2 |k_{2z}|^2}{|\epsilon_2|^2 |k_{1z}|^2} \left(\frac{1}{\text{Re}k_{2z}} \sinh 2a + \frac{1}{\text{Im}k_{2z}} \sin 2b \right) \right\}$$

$$+2 \operatorname{Re} \left\{ \frac{1}{2} \frac{\epsilon_1 k_{2z}}{\epsilon_2 k_{1z}} \left(\frac{1}{\operatorname{Re} k_{2z}} \sinh^2 a - i \frac{1}{\operatorname{Im} k_{2z}} \sin^2 b \right) \right\};$$

in air

$$\langle s \rangle_3 = -\frac{c}{8\pi} \operatorname{Re} \int_d^\infty E_{3z} H_{3y}^* dz, \quad (3)$$

with

$$\int_d^\infty E_{3z} H_{3y}^* dz = \frac{-2\pi\sigma k_x}{2|k_{3z}|^2 \operatorname{Re} k_{3z}} \left[\frac{1}{2} (\cosh 2a + \cos 2b) + \frac{1}{2} \frac{|\epsilon_1|^2 |k_{2z}|^2}{|\epsilon_2|^2 |k_{1z}|^2} (\cosh 2a - \cos 2b) + 2 \operatorname{Re} \left(\frac{1}{2} \frac{\epsilon_1 k_{2z}}{\epsilon_2 k_{1z}} (\sinh 2a + i \sin 2b) \right) \right],$$

where: k_{1z} , k_{2z} , k_{3z} are the complex propagation vectors in the z direction in layers 1, 2, and 3; d is the layer 2 thickness; $a = \operatorname{Re}(k_{2z})d$; $b = \operatorname{Im}(k_{2z})d$; ϵ_1 , ϵ_2 , and ϵ_3 are complex dielectric functions of layers 1, 2, and 3; σ is the frequency in wave numbers; k_x is a complex propagation vector in the x direction; c is the speed of light in cm/sec.

Using these equations in conjunction with the full multimedia equation for determining k_x , we calculated the Poynting-vector (magnitude) ratio of air to overlayer for the system under consideration for Cu_2O thicknesses of 500 and 8000 Å. The results as a function of wave number are plotted in Fig. 4. It appears as though the fraction of energy in the film is quite small, and at the regions of interest near σ_{TO} and σ_{LO} the overlayer attempts to expel the energy into the air. Calculations for a 50-Å film show the same type of behavior. This is in contrast to predictions of field bunching in the film in these regions.⁴ Further study is needed to explain the prior error.

As expected, calculations of k_x , the propagation vector in the z direction normal to the direction of propagation, for each layer show that when damping is included the SEW are never purely exponentially damped or oscillating but are rather a combination. In this frequency range, the mag-

nitudes of each component for a layer are comparable enough that neither part is negligible, especially in the overlayer. However, the character predicted by the undamped case predominates.¹⁰ Thus, if one examines the nature of the k_x in the overlayer, it is primarily oscillating for $\epsilon_2 > 1$ and damped for $\epsilon_2 < 1$ (see Fig. 4). The comparable sizes of the oscillatory and damped parts of k_x negate the usefulness of some approximations which assume purely one nature or the other in the film.⁴

V. CONCLUSION

Our studies of surface electromagnetic waves propagating on a Cu-Cu₂O-air system with damping included have shown that structure in the $1/e$ propagation distance as a function of frequency can be explained by coupled modes. The discovery of a second dip in the propagation distance near σ_{TO} for films of intermediate thickness leads to the possibility of a single experiment to detect σ_{TO} and σ_{LO} for an absorbing film.

ACKNOWLEDGMENTS

The authors would like to thank Dr. I. L. Tyler and Dr. D. L. Mills for helpful comments and Dr. W. H. Weber for consultation on computer methods.

*Work supported in part by the National Science Foundation Grant No. NSF-GH-34551 and the Air Force Office of Scientific Research Grant No. AFOSR-74-2654.

¹C. A. Ward, K. Bhasin, R. J. Bell, R. W. Alexander, and I. Tyler, *J. Chem. Phys.* **62**, 1674 (1975); *J. Chem. Phys.* **62**, 4960 (1975).

²R. W. Alexander, Jr., R. J. Bell, C. A. Ward, J. H. Weaver, I. L. Tyler, and B. Fischer, *J. Chem. Phys.* **59**, 3492 (1973).

³E. Burstein, W. P. Chen, Y. J. Chen, and A. Hartstein, *J. Vac. Sci. Technol.* **11**, 1004 (1974).

⁴R. J. Bell, R. W. Alexander, Jr., C. A. Ward, and I. L. Tyler, *Surf. Sci.* **48**, 253 (1975), and references therein.

⁵L. G. Schulz, *J. Opt. Soc. Amer.* **44**, 357 (1954); A. P. Lenham and D. M. Treherne, *ibid.* **56**, 683 (1966).

⁶P. Dawson, M. M. Hargreave, and G. R. Wilkinson, *J. Phys. Chem. Solids* **34**, 2201 (1973).

⁷D. N. Mirlin and I. I. Reshina, *Fiz. Tverd. Tela* **16**, 2241 (1974) [*Sov. Phys.—Solid State* **16**, 1463 (1975)].

⁸R. W. Alexander, R. J. Bell, D. Bryan, C. A. Goban, M. Davarpanah, and K. Bhasin, *Bull. Amer. Phys. Soc.* **20**, 419 (1975), and to be published; J. Schoenwald, E. Burstein, and J. M. Elson, *Solid State Commun.* **12**, 185 (1973); J. D. McMullen, *Solid State Commun.* **17**, 331 (1975), and private communication.

⁹R. J. Bell, R. W. Alexander, Jr., W. F. Parks, and G. Kovener, *Opt. Commun.* **8**, 147 (1973).

¹⁰C. A. Ward, R. J. Bell, C. A. Goban, K. Bhasin, D. Begley, M. Davarpanah, and R. W. Alexander, *Bull. Amer. Phys. Soc.* **20**, 418 (1975).